2014

Elastic Behavior of Oligolamellar Structures

Scott G. Patterson
University of Vermont, sgpatter@uvm.edu

Elastic Behavior of Oligolamellar Structures

Scott Patterson

April 28, 2014

Advisor: Dr. Yves Dubief

University of Vermont Honors Thesis

Abstract

Synovial fluid provides essential boundary lubrication for diarthrodial joints including the hips, knee, and many other joints in humans. While the structure, molecular components, and properties of synovial fluid are relatively well understood, several theories exist for the mechanism of lubrication. Multilamellar phospholipid structures are believed to be an essential part of the lubricating mechanism, yet the study of the mechanical properties has received little attention from the scientific community. Here we investigate the elastic response of multilamellar phospholipid structures under anisotropic compression using coarse grain molecular dynamics. Various hydration levels are considered in order to develop a relationship between hydration and rupture pressure. This is then used to describe membrane elasticity in terms of hydration. Two regimes of elasticiy are found. Additionally some variation is found between current LAMMPS simulations and previous studies conducted in Gromacs.

Introduction

Human joints are typically classified into three types: synovial or diarthrodial joints, amphriarthroses, and synarthroses. Synovial fluid is found only in the first of these joints. However, synovial joints represent many of the major load bearing joints for humans and other mammals including the hips, knees, inter finger joints, and many others. Various joint geometries include ball and socket, hinge, saddle and plane joints are also lubricated by synovial fluid.[1]

Articular joints generally consist of a synovium, ligaments, tendons, and joint nerves. Certain joints will also include bursae and menisci. The synovium is the thin membrane lining the joint cavity. The synovium separates the joint capsule and internal fluid filled cavity. The tendons, ligaments, nerves, bursae and menisci all aide in the proper function or motion of the joint. Various configurations of these components are capable of providing biomechanical support for a lifetime. Through a human lifespan this system is able to maintain proper lubrication without any means of lateral pressure other than viscous forces. Yet the joint system is capable of resisting anisotropic compression for sustained periods of time all while maintaining an extremely low coefficient of friction. The combination of these properties is well beyond the capabilities of modern mechanical joints in terms of durability, longevity, flexibility, and strength. [1]

As these joints represent such important parts of our body, the understanding and prevention of damage to these joints is crucial. Osteoarthritis (OA) or degenerative joint is one of the more prevalent joint problems. OA affects 3.6% of the global population. As osteoarthritis is recognized as damage to the articular cartilage within a joint, treatment and prevention can be aided through further understanding of the lubrication methods within a joint. Both natural and synthetic solutions to joint diseases must fit into the overall scheme of lubrication.

Corrective medical benefits from further understanding of synovial fluid are not limited to

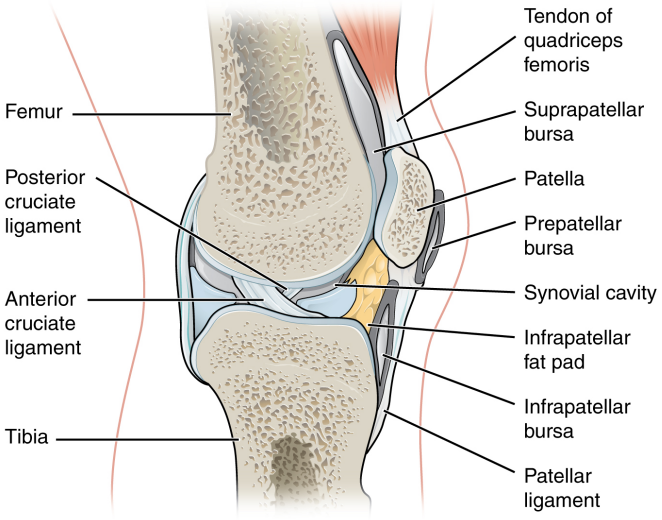

Figure 1: Diagram of knee joint.[2]

treatment and prevention of osteoarthritis. The development and characteristics of prostheses can also be aided through further understanding of the mechanism of lubrication. Wear remains an important concern for most prostheses and medical implants; however, *in vivo* wear is somewhat variable. Some implants will wear quickly while others show considerable improvement relative to *in vitro* testing.[3] Further characterization requires greater understanding than just the lubricant properties. The actual mechanism of lubrication must be studied in order to recognize which situations will maintain natural lubrication and which will require synthetic alternatives. As the life expectancy of humans continues to increase, these technologies will become increasingly important.

Beyond medical implications, synovial fluid provides an amazing target for biomimcry. Most fluid lubrication is accomplished through three different methods: hydrostatic, hydrodynamic, or boundary lubrication. In hydrostatic lubrication, the surface interaction is separated by a fluid film. The presence of this film is maintained through pressurization. Hydrodynamic lubrication achieves reduced friction through the distribution of a viscous fluid via movement of the parts. The limitation of this mode arise from the fluid drain that occurs when the part is stopped.

Wear of the parts will occur whenever the movement is restarted. Boundary lubrication is generally accomplished through coating materials. A thin layer is applied to each surface in order to change the dynamics of the solid-solid interaction. Each of these lubrication schemes has its benefits and downfalls.

Synovial Fluid

Synovial fluid is a non-Newtonian clear or pale yellow fluid contained in small quantities in all diarthredral joints. Synovial fluid is similar in components to blood plasma but does not contain clotting factors or haemoglobin[4]. Total protein content is less that blood at approximately 20mg/mL (2%). Constituents are either derived from blood, secreted from the synovial membrane, or derived from catabolism of the joint. Small molecules such as ions and non-electrolytes diffuse into synovial fluid through capillary permeability. Thus they are found in relative equilibrium between blood and synovial fluid. One exception to this diffusion is glucose, which may be actively pumped into synovial fluid.[5] Due to the larger sizes of proteins, no equilibration occurs. Approximately 63 cells/mm^3 are contained in synovial fluid.[6]

Hyaluronic acid (HA) is one of the primary constituent secreted from the synovial membrane. HA is a high molecular weight glycosaminoglycan (GAG) has been attributed with the high viscosity of synovial fluid as well as many of the lubricating properties.[7][8] Hyaluronic acid has been shown to independently reduce friction relative to a simple saline solution; however, it does not reduce the coefficient of kinetic friction to the level of healthy synovial fluid.[9] Mild digestion by the catalyst hyaluronidase reduces the viscosity of synovial fluid yet does not significantly affect the coefficient of friction.[10] Additionally, isolating the hyaluronate-free fraction shows that the lubricating component of synovial fluid is in the protein fraction rather than the hyaluronate fraction.[10] Hyaluronic acid is also an excellent lubricant under low load conditions, but provides no lubrication under higher loading.[11] Approximately 2mg/mL of HA is contained in the human knee.[12]

Proteins founds in synovial fluid are generally filtered across the synovial membrane. Of the proteins in synovial fluid, albumin is found in the largest quantity.[13] Another large percentage of proteins are either bound or loosely associated with hyaluronic acid.[14] Approximately 0.5% of the protein is the lubricating glycoprotein lubricin or Proteoglycan-4 (PRG-4).[15] Lubricin deficiency in mice and humans resulted in higher levels of friction in joints.[4] This protein may act as a carrier for phospholipids[16] or aide construction of supramolecular structures[4].

Synovial fluid aids in nutrition, protection and lubrication of the articular surfaces in diarthredral joints. Articular cartilage is avascular and thus requires diffusion of nutrients from synovial fluid.[17] Nutrient transport and waste export may be aided by cyclic loading of joint acting as a pump.[18] This effect is believed to be especially important for larger molecular weight solutes. Synovial fluid plays an important role for the lubrication of cartilage surfaces and soft tissue. The hyaluronic acid component is considered essential for soft tissue lubrication.[19] However, loading on soft tissues is significantly less than gate pressure of approximately 1.3MPa[20] where HA is less effective as a lubricant. Additionally, supramolecular structures bounding the synovial fluid may provide barriers to protect collagen fibers in articular cartilage from coagulation protein in the fluid.

Lipids constitute 2mg/mL(0.2%) of the wet weight of synovial fluid. Of this percentage, approximately 32.5% of the constituent lipids are phospholipids. Phospholipids may play an essential role in boundary lubrication of diarthrodial joints.[21][11] Some of the identified phospholipids in synovial fluid include sphingomyelin, dipalmitoyl phosphotidylcholine(DPPC) and dioleoyl phosphotidylethanolamine (DOPE).[4] Various phosphotidylcholine lipids have been found to be the major component (45%). DPPC composes approximately 14.8% of the total constituent

phospholipids.[4][22] Additionally, phospholipids have been found to change concentration during fracture and disease.

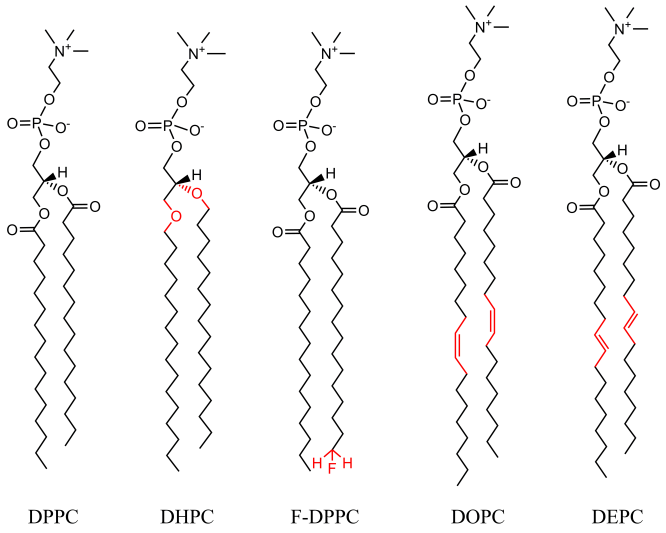

Figure 2: Molecular arrangements for several different phosphocholines.[23]

Osteoarthritis

Osteoarthritis or degenerative joint disease is characterized by degradation of the articular cartilage. However, osteoarthritis also effects subchondral bone, ligaments and muscles, joint capsule, and the synovial membrane.[24] This damage causes bony growths and irritates soft tissue. In turn this causes inflammation and cytokine production that increases cartilage damage. Full osteoarthritis is characterized by full loss of thickness. Early onset is divided into four grades.[25] OA affects 250 million people globally or 3.6% of the population. Synovial fluid is seen to act more newtonian in diseased joints.[26]

Current osteoarthritis cure and treatment is relatively limited. Certain treatments are available for pain reduction, but have little to no effect on retardation of the disease or regeneration of healthy cartilage.[27] These treatments typically include lifestyle changes, such as weight loss, or non-steroidal anti-inflammatory drugs (NSAIDS). Other non-surgical treatments include injections of glycosaminoglycans such as chondroitin sulfate or hyaluronic acid.[12] Total joint replacement is the last resort for treatment of OA patients.

Due to the limited treatment options and incomplete understanding of the disease, further advances in the tribology of synovial fluid may suggest alternative treatments, diagnosis, and prevention methods.

Articular Joint Lubrication

Healthy articular joints are an impressive biological mechanism that preserve effortless and painless movement over a lifetime while experiencing high stresses and impacts. As synovial joints exhibit low metabolic turnover [28][29][30], lubrication rather than regeneration is essential for this longevity. Of the fundamental mechanisms of lubrication, fluid film and boundary are believed to be the most important for joint health. This lubrication is dependent on the loading and kinematics of the joint, properties of the articular cartilage, and chemical and rheological properties of synovial fluid.[31] The interaction between cartilage and synovial fluid is one of the most important of these properties.

Joint lubrication can be modelled as a plane bearing with two parallel surfaces. The limits of synthetic boundary lubrication for this model are a coefficient of kinetic friction (COF) of approximately $\mu = 0.04$ for Teflon.[3][16] In contrast, under constant loading synovial fluid is still able to maintain a COF in the range of $\mu = 0.005$.[3] The unique ability to maintain this low level of friction under continual pressure of up to 1.3MPa has not been match in synthetic systems.

Proper lubrication minimizes two parameters: the wear of the system and the friction. Different types of lubrication are characterized by the distance between surfaces and the substance providing lubrication. Fluid lubrication can be divided into boundary lubrication, in which the surfaces occasionally contact, and hydrodynamic or hydrostatic lubrication, in which a film of pressurized fluid separates the surfaces. Hydrodynamic and hydrostatic are divided based on the movement of the surfaces. Typical engineering

lubrication utilized hydrodynamic lubrication as lower wear and friction can be achieved. Thus a machine experiences the highest levels of wear during the initial start-up or restart as the velocity has not achieved a magnitude large enough to transition from boundary to hydrodynamic lubrication. Additional substances are added to achieve low friction in the boundary and hydrodynamic regimes.

Hydrodynamic lubricating films generally are between $1 - 25\mu$m.[32] Continual motion of the bearing surfaces is required in order to maintain the film thickness. When the surfaces are fully separated, hydrodynamic lubrication generally achieves the lowest levels of friction and wear. A subcategory, elastohydrodynamic lubrication, is characterized by high pressure (1GPa) and solid surfaces that deform elastically. Behavior under these conditions differs from bulk properties. Hydrostatic lubrication is another fluid film lubrication. The film is typically contained via externally provided pressure. Hydrostatic lubrication is most common for low speed, high load application.

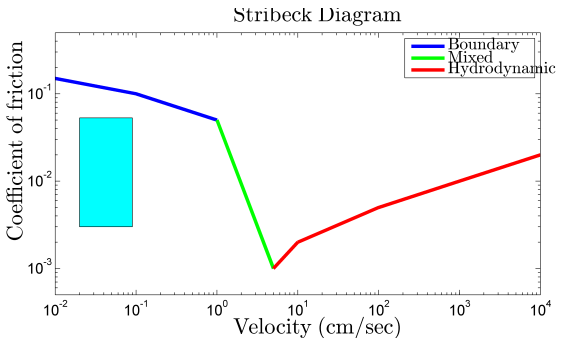

Figure 3: Stribeck diagram. Typical range of operation for mammalian joints shown in cyan.

When the surface separation is lower than this boundary lubrication is predominant. Boundary lubrication is dependent on the adsorption of chemicals into the surfaces rather than the bulk properties of the fluid. This lubrication can operate through several mechanisms such as a sacrificial layer, shear resistant layer, low shear interlayer, friction modifying layer, or load bearing glasses.[33] Solid lubricants such as graphite and molybdenum disulfide[34] are common due to the laminate structure that shears easily. Synthetic surfactants that adhere to the bearing surfaces also provide effective boundary lubrication. However, many are extremely toxic.[35]

Lubrication within articular joints consists of several of the fundamental mechanisms. Taking the knee as an example, five different regimes of lubrication can be considered. During prolonged stance, boosted lubrication is prevalent. In the heel strike phase of a normal gate cycle, lubrication occurs via squeezed film. The weight transfer phase is then characterized by elastohydrodyanmic lubrication. The toe off is a combination of boundary, weeping, and elastohydrodynamic lubrication. Finally, the swing is hydrodynamic lubrication.[36] Weeping lubrication is characterized by the extruding of synovial fluid from the cartilage surface during loading. This form of hydrostatic lubrication is significant in joints.[10] Squeezed film operates on the principle that pressure in joints pushes the fluid film out of contact areas. This creates a pressure gradient which can maintain the fluid film. Boosted lubrication is theorized based on the pores in the articular cartilage which contain synovial fluid. This creates a holey network of fluid film regions separated by regions of boundary lubrication. During the swing, the structure and porosity of the cartilage creates large drag forces that form a pressure gradient. This pressure gradient helps to temporarily maintain a fluid film for hydrodynamic lubrication.[37][4] Under these conditions, fluid film is the predominant mechanism for lubrication.[4]

Due to the ability of fluid films to achieve appropriate friction levels (Figure 3), research has concentrated on isolating components that may act as boundary lubricants. Analysis of the fluid secreted from cartilage show a composition of mostly water and electrolytes.[38] Therefore the boundary lubrication factor is contained in synovial fluid.

Examination of synovial fluid via microfiltration and enzymatic digestion implicates hyaluronic acid as a critical component of the lubricating

mechanism.[39] HA determines the viscosity of synovial fluid, but has limited lubricating ability at high loads. Isolation of components through enzymatic digestion indicated that the protein fraction was also essential for lubrication.[10] Isolation of the hyaluronic acid fraction showed little reduction in friction. Further evaluation lead to the isolation of a glycoprotein termed lubricating glycoprotein (LGP) or "lubricin".[15] The low percentage of the molecular weight attributable to proteins indicates that the essential role may be as a carrier or anchor instead of active lubricant. Digestion by phospholipase has been shown to remove[40] or preserve lubricating ability[41].

The role of lipids in boundary lubrication of joints was first identified by Little et al.[42] Rinsing articular cartilage with fat solvents or lipases caused significant increases in friction. Hills has been a major supporter of lipid as a critical component of joint boundary lubrication.[43] Recent studies have also identified a layer of lipids coating the surface of articular cartilage.[44] It is suggested that destruction of this layer leads to OA onset.

Further study of lubricin through thin-layer chromatography and phosphorous determination demonstrated that 12% previously unidentified is actually phospholipids.[16] Thus the ability of lubricin to coat surfaces in boundary layer lubrication may instead be a property of lipids as a similar percentage of lubricin adheres to cartilage surfaces. This result along with the examination of surface active agents on cartilage[45] has lead to the belief that lipids are the active boundary lubricant in synovial fluid. These lipids are further labelled as surface active phospholipids (SAPL).

Boundary Lubrication

Boundary lubrication is very different from hydrodynamic lubrication. The quality of lubrication is independent of the fluid film properties, such as viscosity, and is independent of the surface shape. Instead surface chemistry is essential for determining the friction and wear associated with a boundary lubricant. Surface chemistry is characterized by the non-homogeneous regime of material around the interface. This manifests as in interfacial energy such as surface tension at a water gas boundary. Surfactants or surface active agents modify this surface energy. Surfactant location at an air-liquid interface is characterized by reduced surface energy.[46] For solids, surfactants must actively bind with the solid interface. This binding can drastically alter the properties of the solid.[43]

Interfacial energy is significantly altered by amphipathic substances. With both a hydrophillic (water loving) and hydrophobic (water hating) region, amphipathic molecules naturally aggregate on water and hydrophobic surface boundaries. Synthetic surfactants will often form multiple layers or multilamellar structures[47][48] and can be effective boundary lubricants when the structure is preserved.

Surfactants are seen in many different industries. Detergents and emulsifiers are some of the most common; however, additional applications include corrosion inhibition, water repellency, permeability modification, viscosity modification, biological defense, and release.[49] Effective boundary lubrication by surfactants is characterized by chemiadsorption to the surface, adsorption quantity to form monolayer, monolayer cohesion, and availability of replacement.

Studies of biological surfactants are commonly focused on the lung. Several different experiments suggest the existence of biological surfactants and their importance.[50] The primary pulmonary surfactant has been identified as dipamitoyl phosphocholine (DPPC).[51] Hills significantly expanded consideration of surfactants for their role in pleurae, gas and solute exchange, and lubrication of surfaces.[11][20] Highly surface active lipids are limited to sphingolipids and phosphoglycerides. Due to the negatively charged nature of many surfaces, biological surfactants are easily adsorbed. For phosphocholines, the positively charged quaternary ammonium serves as the cation for adsorption. Cohesion occurs naturally in phospholipids, but is reinforced by

the addition of other cations. Adding calcium or sodium cations interspersed among phosphocholines pulls together the phosphate group to build a stronger mesh. The fatty acids bonded to the head group also show similar properties, such as chain length (C_{16} and C_{18}), as effective synthetic lipid lubricants.

SAPL is an effective lubricant in certain experimental setups [11][19] yielding friction reductions of up to 70%. Glass on glass explant were used either at atmospheric or under significant pressure. Yet, alternative results suggest SAPL causes no reduction in friction independently or relative to a HA and lubricin solution in others.[9] Most studies supporting SAPL lubrication indicate that SAPL absorption into the cartilage may partially be responsible for the boundary lubrication.[7] Phospholipids have been found to act as effective lubricants for pleural surfaces.[52] Visible evidence has also been provided of oligolamellar phospholipid structures present at the articular cartilage interface.[20][53][54][55] Additionally, SAPL has been found to aggregate onto some artificial joints in a similar fashion.[56] It is suggested that the lamella may act as sacrificial layers in a similar manner to solid lubricants.[20] In addition to the lubrication, the absorption of SAPL at the cartilage surface helps to protect the collagen fibers from the thrombin protein present in synovial fluid.

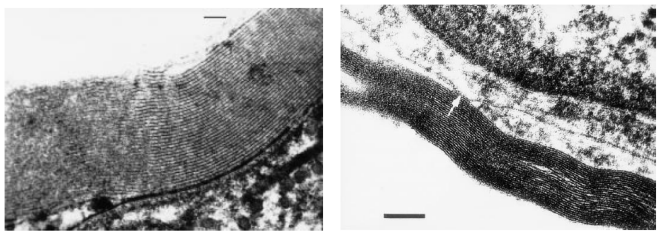

Figure 4: Multilamellar structures on abdomen wall (left) and pleural surfaces (right).[20]

Interactions between hyaluronic acid and phospholipids also shows interesting results regarding lubrication. This interaction is characterized by the creation of supermolecular structures within synovial fluid. Via spectroscopy, hyaluronic acid chain flexibility was seen to increase in the presence of DPPC.[57] This behavior is interpreted as competition for the hydrophobic sites of hyaluronic acid by the DPPC molecules. The competition leads to decreases HA interchain interactions and therefore increases chain flexibility.[7] Further advances are seen via *in vitro* studies of HA and DPPC interactions through negative staining and rotary shadowing electron microscopy. HA and DPPC were seen to form stable supermolecular complexes.[7] In different experiments this structure was found to be either large, holey interconnected membranes connected with HA strands[58] or cylindrical 12nm "rollers" or a complex holey interconnected membranes.[7] The existence of cylindrical rollers is supportive of claims that the surfactants aggregate into lamellar lubricating structures.[7] The hyaluronic acid-phospholipid cylinders also displayed sensitivity to the molecular weight of the HA. In cases of low molecular weight HA, the interactions were considerably less efficient at developing rollers or membrane-like sheets. As hyaluronic acid generally degrades in joint inflammation and osteoarthritis, this dependency on the molecular weight of hyaluronic acid may indicate that the existence of the rollers or membrane-like sheets are crucial for healthy joint operation.[7]

The presence of multilamellar linings and roller structures in synovial fluid suggests a fluid ball bearing as a potential lubricating mechanism. Due to the cohesion of the structures, both oligolammellar cartilage lining as well as phospholipid micelles containing larger and high molecular weight molecules could play important roles in the lubrication of synovial joints. This role is further investigated.

Joint Lubrication Testing

Lubrication of joints is tested in several methods. These generally are comprised of 'arthrotripsometers' which are *in vivo* testing using reciprocating motion or pendulums. The Stanton pendulum measures energy loss per cycle and can be used to characterize lubrication type. Boundary lubrica-

tion maintains a equal drop while hydrodynamic lubrication the loss declines with amplitude of the pendulum. Various studies can be conducted using Stanton pendulums by eliminating certain parts of the studied joint.

The second common method for testing lubrication is using explants and rubbing surfaces against each other. Common surfaces include cartilage and glass. By evaluating lubrication outside of the biological system, individual components may be studied either through removal from more complex solutions, attempted isolation, or synthetic construction. This also provides additional benefits through simplification of the system avoiding the ploughing effects experienced during pendulum swings. Various tribometer configurations are utilized such as pin-on-flat, pin-on-disc, annulus-on-flat, and disc-on-plate.[59]

Tribological testing of synovial fluid is limited due to the small quantity of synovial fluid in joints and the high possibility for contamination. Bovine and equine synovial fluid are most commonly studied. *Ex vivo* synthetic build-up of synovial fluid has also proven difficult.[60]

Molecular Dynamics

Molecular dynamics (MD) provides an opportunity to examine properties on an entirely different level than experimental testing. Due to difficulties with quantity, contamination, and isolation of substances MD is well suited for studying the lubrication properties of synovial fluid. While examination of a fluid film utilize conventional computational fluid dynamics and examine properties such as viscosity, boundary lubrication is more generally suited to molecular dynamics. The full scale of a fluid film is beyond currently available computing power; however, relevant domain sizes can be examined for boundary lubrication. Additionally, as the surface chemistry and molecular interactions become critical to the behavior of lubricant, full realization of the molecular structure is an important supplement to the bulk properties of the fluid.

Among the many benefits of computation studies is the ability to isolate certain components and develop continuum level models for their behavior. These models can provide additional insight while also suggesting areas for future experiments without the confounding variables present.

Molecular dynamics solves Newton's laws for a n-body problem and iterates forward in time in order to characterize larger behaviors in terms of atoms or molecules. Each molecule or bead is assigned certain parameters in order to associate behaviors in simulation with real world interaction. The most simple of these models is the Lennard-Jones (LJ) bead which interacts with other non-bonded molecular beads based on two parameters (ϵ, σ) and the energy potential equation

$$E_{LJ} = 4\epsilon \left[\left(\frac{\sigma}{r}\right)^{12} - \left(\frac{\sigma}{r}\right)^{6} \right] \quad r < r_c \qquad (1)$$

where r is the radius and r_c is the cuttoff radius. The first term accounts for short range interactions such as electron overlap and the second accounds tor attractive van der Waals and dispersion forces. These parameters are evaluated through experimental results, theoretical evaluation, or fitting of other parameters. Addition interactions occur via bonds, angles, dihedrals, dipoles, and electric potentials. Bonds and angles in simple models rely on Hookean linear and torsional springs.

Various methods within solvers are used to reduce the computational load of molecular dynamics.

Coarse Graining

Coarse grain molecular dynamics (CGMD) provides two primary advantages over standard atomistic simulation. First, longer time steps can be used for the simulation since some of the micro interactions have been smoothed. Second, coarse graining reduces the number of bodies to compute. Due to limited computing power as well as desire to simulate larger domains, coarse graining has become a standard practice. Several different

schemes exist developed from physical chemistry and parameter matching. For each model, certain elements are preserved from atomistic and experimental result while others suffer.

Two phospholipid coarse graining schemes are considered: the MARTINI force field and the ELBA (ELectrostatics BAsed) potential.[61][62] Both schemes were developed for coarse grain simulation of lipid bilayers. The MARTINI force field has be used extensively within the Gromacs solver as a simple coarse graining solution. This coarse graining scheme was implemented for previous studies of multilamellar structures under anisotropic compression(unpublished data Dubief, Cowley). Both schemes group atoms as larger Lennard-Jones beads with several molecules per bead. In the ELBA forcefield, the 138 atoms composing a dioleoylphosphatidylcholine (DOPC) molecule are reduced to 15 coarse grain sites. The MARTINI forcefield is developed from systematic parametrization based on thermodynamic data and reinforced with experimental partitioning data. This modelling focus is the fluid phase of lipid bilayers.[61] ELBA is based on the explicit representation of electrostatic based potentials and replication of a specific dielectric constant. Also important during development was the use of the standard Lorentz-Berthhelot mixing formulae utilized for atomistic simulation as follows:

$$\sigma = \frac{\sigma_i + \sigma_j}{2} \quad \epsilon = h\sqrt{\epsilon_i \epsilon_j} \tag{2}$$

for defining interactions between LJ-bead i and j with a scaling factor h.[62]

The ELBA force field offers several advantages over MARTINI or other schemes. One important difference between these two potentials is the treatment of water molecules. MARTINI groups four water molecules as a single LJ bead. ELBA treats each molecule as a LJ bead. Although either potential serves certain purposes, the more refined beads utilized for the ELBA potential provide additional information regarding permittivity of lipid membranes.

ELBA also offers possibilities for working in multiscale or dual-resolution domains. The parameters and mixing rule in the ELBA force field allows for simultaneous use of atomistic regimes and coarse grain regimes. This increases flexibility as study is not limited to those molecules previously evaluated with regard to the coarse graining scheme. In this manner, addition of cations or other non-electrolytes among phospholipids is possible in ELBA. Adding these particles using the MARTINI forcefield is considerably more difficult as a new coarse grain bead would be required. Interaction parameters must be determined from previous data or experimental results.

Another important advantage of ELBA is the accurate lipid dynamics.[62] With most coarse graining schemes, parameters such as the mean squared displacement and lateral diffusion are altered. Due to these changes the simulation time step must be carefully evaluated in schemes such as Martini.[61] Atomistic simulation and comparison is often necessary in order to evaluate the differences in time scale due the nature fo the coarse graining scheme.

Solvers

Although a multitude of many body solvers and programs have been developed for use with molecular dynamics, two common programs were utilized: Gromacs and LAMMPS.

Gromacs (GROnigen MAchine for Chemical Simulation) was initially developed for molecular study of proteins and other biological models. Expansion into other regimes has occurred due to the high level of computational optimization and forcefield flexibility added to the initial solver.

LAMMPS is the Large Atomic/Molecular Massively Parallel Simulator. Developed by Sandia National Lab this program provides significantly more flexibility relative to Gromacs. Due to the nature of the program for general study rather than the focus on biological molecules, important features for engineering studies are added. For instance, while basic stress states are relatively easy to replicate in both solver, LAMMPS

provides considerably more advance possibilities.

Both solvers operate on similar essential principles yet provide different levels of optimization and flexibility. Ideally using the different solvers with identical parameters would produce similar results.

Bilayer Properties

Lipid bilayers have been the subject of a vast numbers of studies both experimentally and computationally due to their importance in cell membranes. However, the critical properties for membranes differ significantly from those that are considered important for the boundary lubrication found in synovial joints. Thus new parameters and methods of determining these parameters are necessary.

Typical evaluation of lipid bilayers includes the electrostatic potential, the electron density, and lateral pressure profiles. Additionally parameters considered are the area compressibility modulus, bending modulus, permittivity, and lateral diffusion. These properties can be evaluated both through experimental methods with varying degrees of accuracy and through computational study. Typical evaluation of coarse graining schemes and forcefields considers differences in these characteristics in order to isolate limitations and benefits of the model.

In relation to synovial fluid many of these parameters provide inadequate information as they do not take into account important properties and differences. One of these key parameters is the hydration level (Eq. 3).

$$h = \frac{\text{Number of water molecules}}{\text{Number of lipids}} \tag{3}$$

Based on the level of hydration different types of interactions occurs. This is especially important for low hydration levels due to the effect of hydration forces (Eq. 4) when surface spacing is small. Hydration force can be expressed as

$$P = P_0 e^{-\frac{H}{\lambda}} \tag{4}$$

where P_0 is the force amplitude, H is the surface spacing, and λ is the decay length.

In experimental studies, bilayers are often examined through monolayer vesicles subjected to known stresses. Osmotic swelling is often used to develop tension. This allows determination of the area compressibility modulus and the bending modulus.[63] Methods using atomic force microscopy (AFM) have taken place more recently. Reliable parameters are difficult to evaluate due to the confounding effect from smoothing of membrane undulations.

Methods

Elastic behavior of multilamellar structure is studied through coarse grain molecular dynamics. Several different hydration levels are considered. Domain area is taken to be a small slice of the multilamellar structure lining the articular cartilage of synovial joints. As such a three dimensional periodic boundary is instituted for all simulations in order to simulate the larger structure and multiple layers. This small domain is assumed to be distant from cartilage surface as no artificial surface is created in the simulation. Elastic behaviors of this structure are characterized through increasing anisotropic compression. Key parameters varied between studies include the number of lipids and the hydration level or number of water molecules per lipid. Important characteristics for evaluation include the area per lipid as well as the final rupture pressure.

Using NPT coarse grain molecular dynamics in the Gromacs and LAMMPS solvers, the behavior of oligalamellar structures is investigated. Preliminary investigation is conducted in Gromacs using the MARTINI force field and coarse graining scheme. In a three dimensional periodic domain, a hydrated membrane is subject to controlled anisotropic compression using Nose-Hoover thermostat at 310K (body temperature). A semi-anisotropic Parrinello-Rahman barostat is maintain directions parallel to the membrane at atmospheric pressure ($P_{\|} = 0.1$MPa) while in-

creasing pressures are applied to the perpendicular direction ($P_\perp$) with steps of 1MPa initially and 2MPa when the pressure is above 10MPa. A time step of 40fs is used. The symmetric pressure tensor can be expressed as

$$P_{IJ} = \frac{\sum_k^N m_k v_{k_i} v_{k_j}}{V} + \frac{\sum_k^N r_{k_i} f_{k_j}}{V} \qquad (5)$$

where the first term use kinetic energy tensor and the second use the virial tensor.

Input arrangements consist of coarse grain models of dipalmitoylphosphatidylcholine (DPPC) arranged in a bilayer. Coarse grain water beads are placed above and below the bilayer construct. Hydration levels of $h = 16, 32, 64, 128, 512$ (Eq. 3) are considered

Later investigation is conducted in LAMMPS using the ELBA potentials and coarse graining scheme. In a three dimensional periodic domain, a hydrated membrane is subject to controlled anisotropic compression using Langevin thermostat at 303K. The damping time scale is set as $\tau_T = 0.1$ps for initial NVT equilibration. Input structures equilibrate prior to application of a barostat for 0.5ps. Upon barostat application, a semi-anisotropic Berendsen barostat maintains directions parallel to the membrane at atmospheric pressure ($P_\parallel = 0.1$MPa) while increasing pressures are applied to the perpendicular direction ($P_\perp$). The parallel directions are not coupled. The pressure damping time scale and thermostat damping time scale are set to $\tau_P = 0.5$ps and $\tau_T = 1.0$ps respectively. The simulation time step is 10fs. Simulations are conducted for 20ns at each pressure with maximum pressure increases of 1.0MPa. Pressure is increased until obvious rupture and destruction of the oligolamellar structure. The compressibility was set at $\beta = 4.6 \times 10^{-4}\text{MPa}^{-1}$. Hydration levels of $h = 16$ and $h = 32$ (Eq. 3) are considered. Additionally, different size domains are considered with either 128 or 512 phospholipids.

Input arrangements for LAMMPS simulation consist of hydrated dioleoylphosphatidylcholine (DOPC) lipids arranged in a bilayer.(Figure 5) The coarse grain water beads are placed above and below the bilayer construct. Desired hydration levels are achieved by porous deletion of water beads or addition of water beads outside of bilayer. During addition of beads randomized dipole orientations are used. The initial domain is set as square in the x and y directions with size dependent on the number of phospholipids. For initial equilibration the periodic z boundary is set to give each water bead approximately 0.03nm^3.

Several differences can be noted between the two models. Attempts were made to preserve the conditions between each model but some concessions were required. The choice of phospholipid was based on studies indicating DPPC as the prevalent phosphocholine in synovial fluid. However, ELBA was explicitly parametrized using DOPC. Thus using DOPC provided easier comparison with pas models to verify proper application of the model. The differences between these two molecules is in the chains. DPPC is composed of two palmitoyl fatty acids with carbon chain length of 16 (C_{16}). DPPC is a saturated phospholipid as no double bonds are present in the carbon chains to alter the curve. DOPC chains consist of two oleoyl fatty acids. The carbon chain is of length 18 (C_{18}) and is unsaturated due to the presence of a double bond on he carbon chain.

Additionally, different time steps, temperatures, thermostats, and barostats were utilized. The 40fs simulation for Gromacs was pushing the maximum. Thus for ELBA simulation a more conservative time step of 10fs is required. The choice of thermostats and barostats was based application of simple first order constraints in order to provide effects without significantly increasing computational time. Additionally, limited differences were seen between Berendsen and Parrinello-Rahman barostats for the simulation conditions.[64] Temperature choice was chosen based on early simulations which displayed greater lateral diffusion and permittivity. Thus a lower temperature was utilized in order to attempt to stabilize the membrane.

Data was collected as full coordinate and dipole dumps every 0.1ns. In addition more frequent logging occurred dimensional values, surface tension, mean squared displacement. Profiles were generated for numerical density, electron density, electrical potential, lateral pressure, and radial distribution function every 20ns when the pressure was increased.

Visual Molecular Dynamics is utilized for visualization purposes.[65]

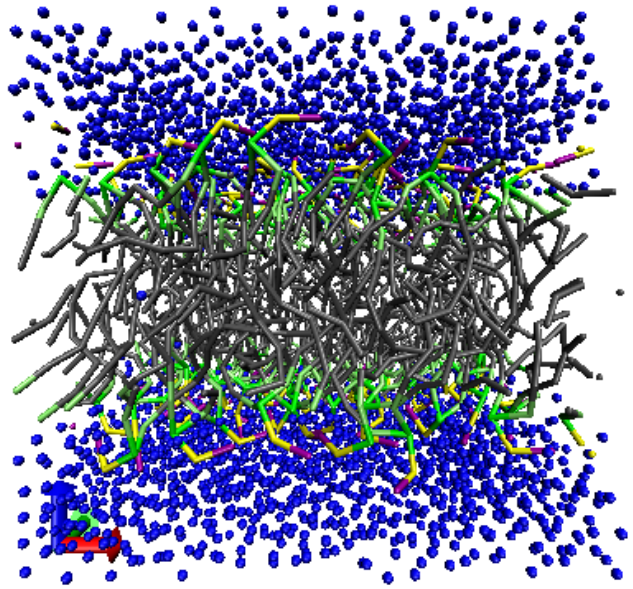

Figure 5: Wrapped input arrangement for 128 DOPC lipids and hydration of 32 waters/lipid.[65] Water shown in blue. Lipids shown as licorice bonds. Coarse grain beads are as follows: purple - choline, yellow - phosphate, green - ester, lime - glycerol, and gray - tail.

Results

Model verification relative to previous studies and experimental data is an important consideration for any molecular dynamic simulation and even more so with a coarse grain scheme implemented. This verification provides a reality check and confirms proper application of the model prior to developing relationships from this scheme. Following model verification, the anisotropic pressure buildup is evaluated with further results regarding the rupture pressure and its relation to hydration level. Additionally elasticity relationships, undulations, peristaltic fluctuations and model comparisons are evaluated.

Table 1: Bilayer parameter comparison. Brahams simulation was used for development of the ELBA coarse graining scheme.[62] Experimental data is from [66][67][68][69][70][71]. Bilayer thickness calculated differently for LAMMPS simulation.

Hyd:#Lip Solver	$A_0(\AA^2)$	$V_0(\mathrm{nm}^3)$	$L_{bl}(\AA)$
16 : 128 Lammps	67.60 $\pm$0.872	1.260 $\pm$0.0019	28.85 $\pm$0.420
16 : 512 Lammps	67.28 $\pm$0.411	1.261 $\pm$0.0097	28.98 $\pm$0.223
32 : 128 Lammps	65.94 $\pm$0.80	1.260 $\pm$0.0021	23.62 $\pm$0.617
32 : 512 Lammps	67.04 $\pm$0.312	1.260 $\pm$0.0094	29.03 $\pm$0.198
Gromacs	60.75		44.4
Brahms	71.95 – 72.82	1.300 – 1.302	32.58 – 34.78
Exp.	67.4 – 72.5	1.292 – 1.303	35.3 – 37.1

Model Verification

Initial LAMMPS simulations conducted at $P_\perp = P_\parallel = 0.1$MPa were compared with previous ElBA studies, Gromacs studies utilizing the MARTINI force field, and some experimental data in order to briefly verify proper application of the ELBA model to the DOPC bilayer. Values compared include area per lipid (A_o), volume per lipid (V_o), and bilayer thickness (L_{bl}) (Table 1). Bilayer thickness is computed from the average glycerol z location rather than the head group due to initial higher water permittivity in early simulations. This problem was corrected but the recorded data remained.

As seen in Table 1 dimensional parameters show reasonable reproduction of experimental values. In contrast to previous ELBA simulations[62], area and volume per lipid are seen to be on the low range of experimental values. Additionally Gromacs simulations at atmospheric pressure are seen to display area per lipid significantly less that either ELBA simulations using LAMMPS or

previous simulations or experimental data. The area per lipid is much more closely replicated for the ELBA forcefield. Although bilayer thickness was evaluated differently between the several models, on can see from figure 6, that bilayer thickness also is correctly reproduced.

Another important note of this model verification is the correlation of values between simulation size. For both hydration levels considered the extracted dimensional parameters are reproduced relatively closely. This is especially true for the hydration level of 16. For all three noted parameters, values are within one standard deviation. The simulations conducted at hydration of 32 show similar results although slightly larger differences are present. All dimensional evaluation shows consistency for area per lipid under decoupled atmospheric compression.

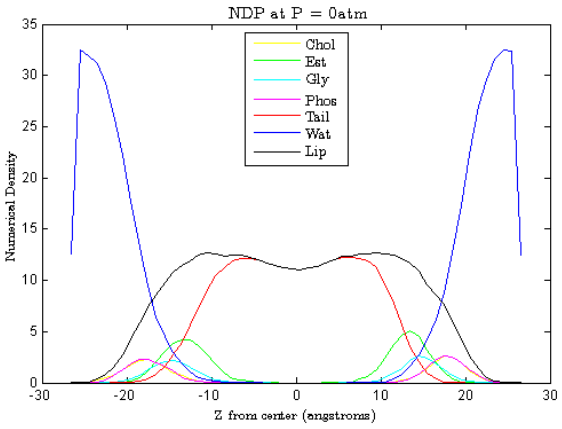

Figure 6: Numerical density profile at $P_\perp = 0.1$MPa at $h = 32$ and 128 lipids.

Model validity can also be evaluated through comparison of the electron density profile shown in figure 7 and the electrostatic potential profile shown in figure 8. Although previous ELBA simulations show some differences relative to experimental data for the electron density[62], the overall magnitude and shape of the curve is similar. This total electron density profile is reproduced with relative accuracy with some errors in the overall magnitude in at the headgroups and the center of the bilayer. Theses results confirm previous limitations of the ELBA force field. The electrostatic potential profile shows some similar characteristics but also significant differences relative to ELBA and atomistic simulation. Relative to atomistic simulations, the electrostatic potential displays strong dependence on the dipole of the ester coarse grain bead. This was also seen in previous ELBA simulations and attributed to the weaker orientation effects with respect to water. Atomistic simulation show electrostatic potential dominated by the contribution from the dipoles of water molecules.[62] The electrostatic potential was calculated as

$$\Psi(z) = -\frac{1}{\epsilon_0}\int_0^z dz' \left[\int_0^{z'} \rho(z'')dz'' - \mu_z(x')\right] \quad (6)$$

where ϵ_0 is the permittivity of free space, ρ is the charge density, and μ_z is the z-projection of the sum of point dipoles. Relative to ELBA simulations, calculated in the same manner, the LAMMPS data shows considerably different electrostatic potential due to the water dipole. The ELBA simulations show a positive electrostatic potential attributed to water in the headgroup region. This causes the overall electrostatic potential to remain above the headgroup charge potential throughout the z profile. Differences in these results may be attributable to the electrostatic potential calculation method. Slices along the xy plane were taken with little regard to the undulations of the membrane. Thus for larger systems in which undulations are present, such as the simulations with 512 lipids, this may result in inaccuracies.

Overall model verification has indicated that some errors are present relative to atomistic simulation and experimental results; however, the general parameters have been successfully reproduced. Confirmation of reproduction and knowledge of potential error sources must be considered when building up pressure.

Pressure Increase

In order to allow for settling after each pressure increase shock, parameters were evaluated

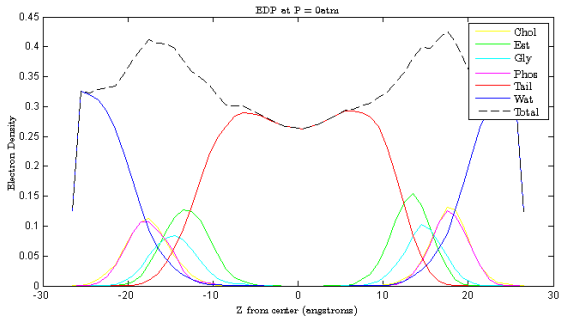

Figure 7: Electron density profile at $P_\perp = 0.1$MPa with $h = 32$ and 128 lipids.

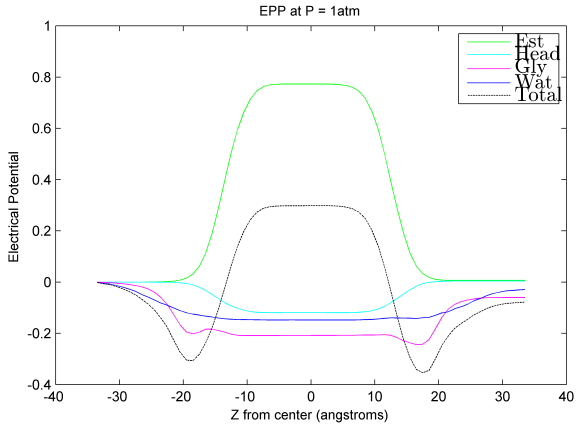

Figure 8: Electrostatic potential profile at $P_\perp = 0.1$MPa, $h = 32$, and 512 lipids.

for the last 10ns of the 20ns pressure hold. As seen through the evaluation of rupture, ideally each pressure should be held for a longer time to allow settling or rupture before adding another shock to the system. However, 20ns was deemed adequate in order to allow for faster computation and more simulation runs. Numerical density, electron density, and electrostatic potential profiles were calculated at each pressure hold. In addition, center of mass, domain dimensions, and bilayer thickness were recorded.

As seen in figure 9, the radial distribution function can be seen to be increasing for greater pressure. This function was calculated for the glycol group, located at the head tail junction, and water molecules. General trends show increasing likelihood of water within close proximity of the glycol group.

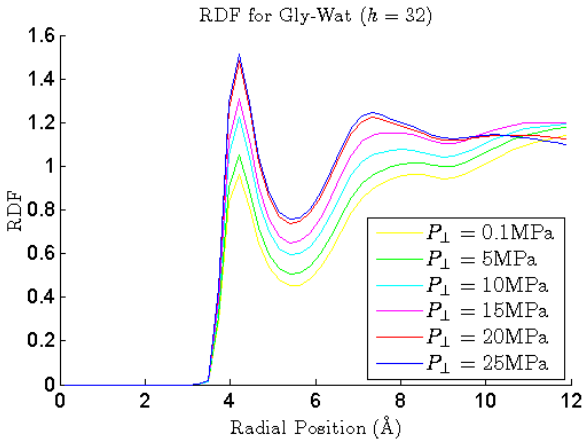

Figure 9: Radial distribution function for increasing pressure at $h = 32$ and 128 lipids.

Additionally numerical density profiles indicate changes as the pressure is increased. Comparing the graphs in figure 10, three items stand out. The first is the total numerical density no longer decreases in the center of the bilayer. This can be directly attributed to the pressure increase causing a more closely packed arrangement. The second change is the greater presence of tail beads interspersed within the glycol and ester groups. The third noticeable change is the greater presence of water in the head groups and early tail. All of these attributes can be explained through

closer packing of the structure as a response to the increased pressure.

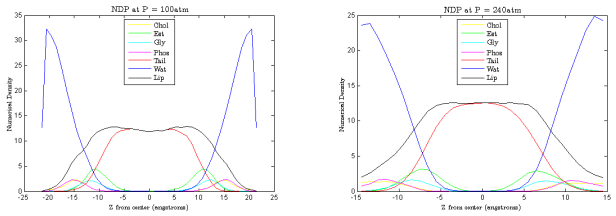

Figure 10: Numerical density profiles at $P_\perp = 10$MPa and $P_\perp = 24$MPa with $h = 32$ and 128 lipids.

Describing Rupture

Rupture of the multilamellar structure at high pressure can be seen in several factors. The most easily noticed is the drastic transition in the organization of the domain. Through full coordinate visualization over time it can be seen the that domain shifts from a compressed lamellar structure. This shift is typically indicated first in a small region with lipid tails changing orientation from along the z axis to in the xy plane. This affect pushes water molecules into the previously hydrophobic region of the bilayer structure and causes additional breakdown. Within a few picoseconds the entire domain of lipids has shifted orientation. This breakdown is also characterized by a significant increase in area per lipid. Numerical density, electron density, electrical potential, and lateral pressure profiles along the z axis also show significant changes.

As a more concrete demonstration of the lipid rupture procedure we can examine the 128 lipid simulation a hydration of 16. As full coordinate dumps were taken ever 0.1ns our evaluation proceeds on that time scale. The initial development is characterized by the formation of a penetration of the lipid bilayer by water molecules. Under lower pressures or atmospheric conditions, these water molecules would be rapidly removed from the bilayer due to the hydrophobic nature of the tails. However, under the considerably higher pressure of $P_\perp = 26$MPa the system possesses far greater instability. It takes about 2ns from the initial pore development until lipid headgroups are reorientated to define the pore boundaries. The pore then remains relatively stable for the remaining 3.5ns before the following pressure increase to $P_\perp = 27$MPa. The increase in pressure further destabilizes the water pore. Instead of the constant size that was maintained for the length end of the lower pressure, the water pore rapidly increases in size. This pore expansion results in the reorientation of lipids in the surrounding region creating pockets of lipids. This effect propagates through the entire domain. Another 7ns are required for the full reorientation of the phospholipids and the division of the xy plane into water pockets lined by lipid headgroups. Also during the full rupture the water pockets freeze. Full rupture takes approximately 14ns.

Due to the close-packing nature of a hexagonal lattice (Figure 12), we can describe the area per lipid as the hexagonal region surrounding the lipid head. This allows characterization of bilayer rupture as a significant increase in area per lipid. Gromacs data and LAMMPS visualizations indicate that rupture occurs when the area per lipid increases by approximately $A_c = 0.5\text{nm}^2$. For area per lipid beyond this values, the physics of the bilayer are significantly altered. This critical area is recognized as a critical parameter in which the packing is no longer tight enough to prevent penetration by water molecules. This designation does not perfectly described exactly when the bilayer will rupture, but is within the range and demonstrates potential for bilayer rupture.

Based on the behavior of the bilayer, we can define a critical rupture pressure P_c as the pressure when

$$A = A_0 + A_c \tag{7}$$

where A is the area per lipid, A_c is the critical area per lipid as previously defined, and A_0 is area per lipid at $P_\parallel = P_\perp = 0.1$MPa.

Effect of Hydration

Hydration has been seen to have a significant effect on the rupture pressure of the multilamellar

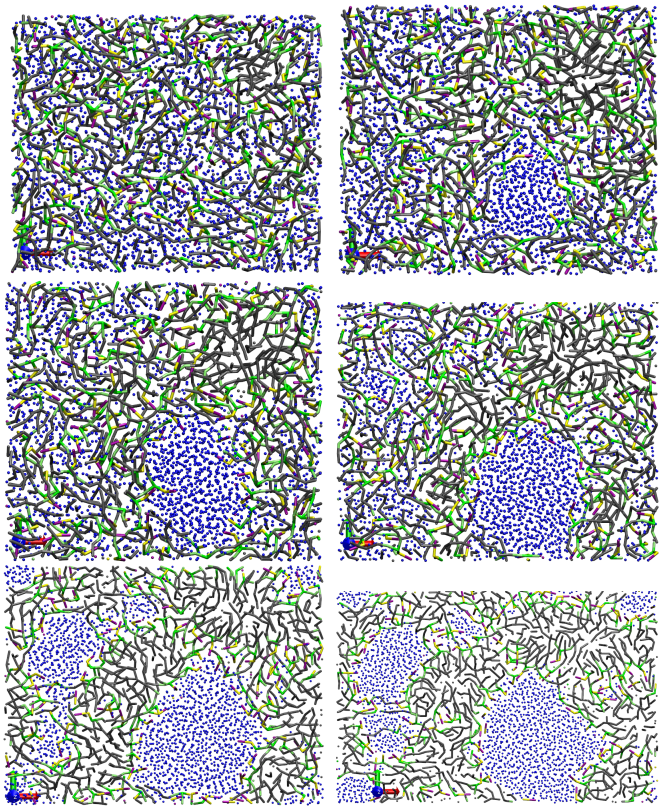

Figure 11: Images displaying rupture process. From top left to bottom right shows the initial pore development, a stable water pore, pore expansion, rearrangement of the head groups, full rearrangement, and further flattening. Pressure increase occurs between the second and third images. Images are looking at xy plane. While bilayer is still intact water molecules are shown between lipids.

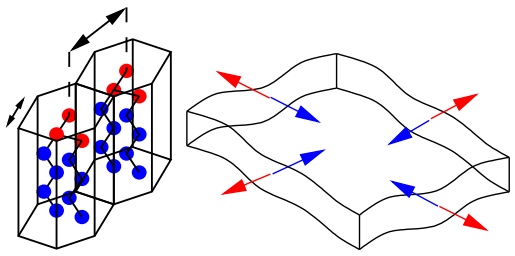

Figure 12: Hexagonal packing structure illustrated (left) and illustration of continuum force balance.

structure. Using Gromacs simulation the relation

$$P_c = P_0 / \left(1 + \frac{h}{h_\lambda}\right) \tag{8}$$

was developed where $P_0 = 40$MPa and $h_\lambda = 26$ are parameters tailored to fit the curve. Theoretically these parameters are explained as the hydration pressure and the critical hydration for the onset of hydration forces. Utilizing these parameters provides a close match for relating critical pressure at low hydration but shows greater error for higher values. Further tailoring of this relationship and theoretical backing is necessary.

Additional simulations at higher levels of hydration should also be conducted in LAMMPS in order to verify this relationship between critical pressure and hydration. Simulations with hydration of 32 ruptured at a higher perpendicular pressure than previously simulation in Gromacs. While this result is not conclusive, it does provide some suggestion that further refinement of the relationship is required.(Figure 13) The differences in phospholipids (DPPC v. DOPC) and temperature may also explain some of these differences.

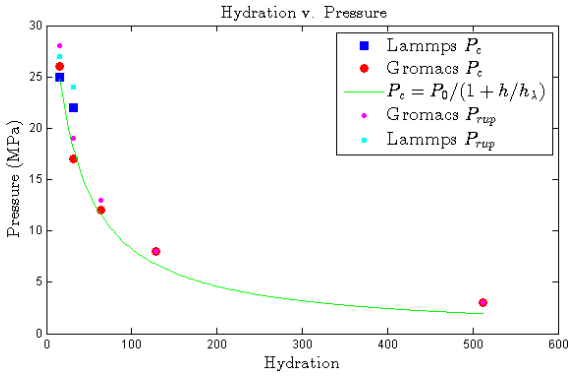

Figure 13: Hydration v. Pressure for Gromacs and Lammps simulations. Developed curve for relation shown in green.

Undulation and Peristaltic Oscillation

Lipid bilayers in simulation display both undulations and peristaltic fluctuations. Undulations

can be measured through the location of the center of mass of the bilayer. Peristaltic oscillations are measured through bilayer thickness fluctuations. Continuum models suggest behaviors of the spectral density function for both of these parameters.

However, both undulations and peristaltic fluctuations are highly dependent on the size of the domain. Smaller domains such as those with 128 lipids, preserve artifacts across the periodic boundary conditions and unnaturally smooth the undulations. Some fluctuations may occur but these are also limited. Due to this nature and the limited size of the simulation domain, full analysis of the fluctuations was not conducted.

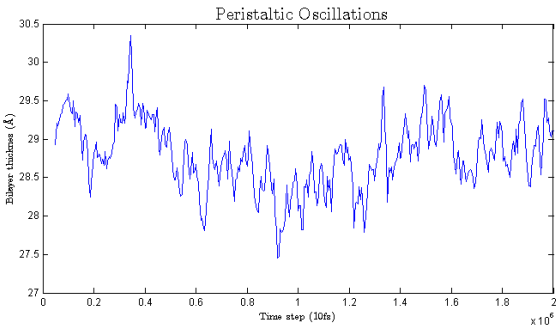

Figure 14: Peristaltic oscillations in bilayer thickness measured as average distance between glycol groups at $P_\perp = 0.1$MPa with $h = 16$ and 128 lipids.

Oligolamellar Elasticity

Phospholipid membranes deform elastically under normal stress. Utilizing a continuum model the elastic energy should reduce to

$$E = \frac{1}{2}k(A - A_0)^2 \tag{9}$$

Opposing this is the work exerted by pressure. This system can be then placed in terms of the energy balance

$$[k(A - A_0)/A_0]A_\perp = (P_\perp - P_\parallel)A_\perp \tag{10}$$

As seen in figure 15 the area per lipid changes in a relatively uniform pattern between different

Table 2: Least squares regression parameters for elasticity regimes using LAMMPS simulation data.

Hydration	Regime	Equation	r^2
$h = 16$	1	$A^* = 0.6143\Pi - 0.0043$	0.4447
$h = 32$	1	$A^* = 0.6809\Pi + 0.0041$	0.6520
$h = 16$	2	$A^* = 1.3452\Pi - 0.345$	0.6856
$h = 32$	2	$A^* = 1.3535\Pi - 0.3317$	0.7739

hydration levels. We can normalize this data using the critical pressure previous defined to get

$$\Pi = \frac{P_\perp - P_\parallel}{P_c - P_\parallel} \tag{11}$$

Utilizing this normalization, the Gromacs data shows two regimes of elasticity with uniform behavior across different hydration values.

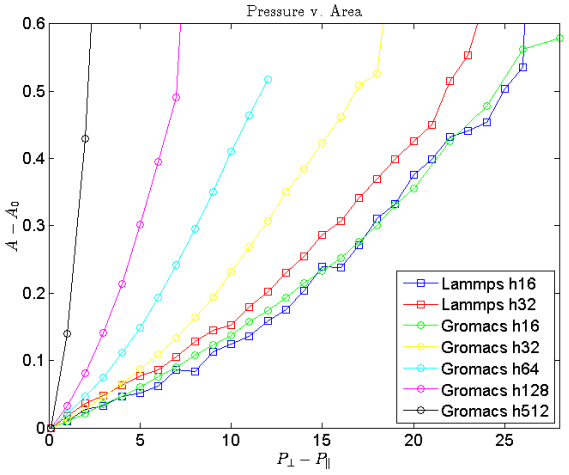

Figure 15: Area per lipid response of bilayer to pressure increases based on hydration. Points off the top of the figure represent rupture.

The elastic behavior seen in figure 16 can be expressed in form of a piecewise function. Utilizing the developed expression for critical pressure based on the hydration level, an expression for the area per lipid is expressed as a function of

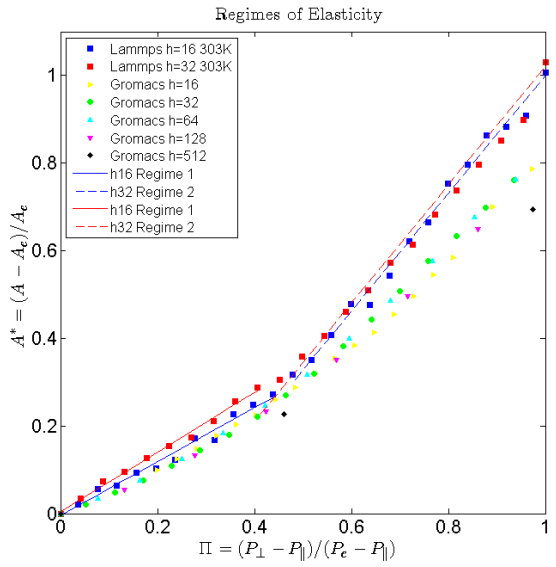

Figure 16: Two regimes of elasticity based on normalized pressure data.

pressure and hydration in the form

$$\frac{A - A_0}{A_c} = \begin{cases} \dfrac{1}{3P_0}\left(1 + \dfrac{h}{h_\lambda}\right)(P_\perp - P_\parallel) \\ \quad \text{for } P_\perp - P_\parallel \leq \dfrac{1}{2}\left(\dfrac{P_0}{1 + h/h_\lambda}\right) \\ \dfrac{2}{3P_0}\left(1 + \dfrac{h}{h_\lambda}\right)(P_\perp - P_\parallel) + C \\ \quad \text{for } P_\perp - P_\parallel > \dfrac{1}{2}\left(\dfrac{P_0}{1 + h/h_\lambda}\right) \end{cases} \tag{12}$$

where h_λ and P_0 are as previously defined and C is a constant offset.

In the case of the LAMMPS simulation results, we see significantly different slope relative to the 1/3 and 2/3 in equation 12. Full least squared regression parameters are shown in table 2. Significant differences in slope is especially evident in regime two of the elasticity behavior. This difference suggests that the universal regimes of elasticity found in previous Gromacs simulation may be dependent on the coarse graining model. However, some ambiguity exists in this regard due to the slightly different configurations of the simulations. More simulations, comparison with atomistic simulation, and if possible experimental backing would be useful to confirm these results.

Conclusion and Future Work

The transition from Gromacs to LAMMPS for modelling multilamellar structures shows some similar results and some differences relative to previous work. The effect of hydration on rupture pressure has been confirmed for low hydration levels. Higher hydration was not considered due to limited computational time and relevance to synovial fluid lubrication. When acting as a boundary lubricant, surface active phospholipids are assumed to be hydrated less than $h = 128$M(Eq. 3). Additionally, the existence of two regimes of elasticity is indicated again. However, the evaluation of the exact relations will require further study. LAMMPS studies showed different slopes than those derived from Gromacs simulation.

While these represent important considerations for the development of continuum models for multilamellar structures, the true importance of these results lays in the future potential of the model. The multilamellar structure has been effectively transitioned to LAMMPS and provided similar results. Further study can now consider different configurations and variables with relative ease. Among the parameters that warrant additional attention are the type of phospholipids and the temperature.

Expanding the domain in several different manners may also show interesting behaviors. The rupture behavior of a single bilayer made into a multilamellar structure through periodic boundary conditions may be different that a true multilamellar structure. Examination of a larger domain via replication in the z direction could provide this result. During single bilayer rupture, changes in orientation of the phospholipids are seen. Larger domains may show recombination of multiple bilayer into a single layer or indicate rupture of only a single layer.

This basic setup could be easily adjusted to more complex non-equilibrium molecular dynamics through the addition of external forcing. Shearing the bilayer structure would provide additional details seen in synovial joints that is not currently replicated in simulation. This would require definition of a triclinic domain from the current system but could be accommodated within the LAMMPS model. Adding shearing or other forces would allow additional description and continuum model development for the boundary lubrication found in synovial joints.

In addition to further advances in the model, certain parameters need to be refined in order to increase the flexibility and applicability. Currently, processing different levels of hydration is relatively difficult. Several changes to the input files would simplify this procedure while allowing for more flexibility. Additional limitation lies in the phospholipid structure in the input file. Ideally, an input file could be created from a single phospholipid. This procedure was followed for an extended period of time but the model did not replicate either previous ELBA simulations or experimental data. The most obvious differences lay in the thickness and permeability of the membrane. Water penetration was occurring at orders of magnitudes higher than seen in experimental membranes. A shift to a less structure input system allowed for proper reproduction of bilayer parameters with very similar simulation structure. However, this locked in the lipid in consideration for the current time.

Additional streamlining of the pressure increases and output generation may be helpful. Among the most important considerations is refining tools allow for consideration of undulations in the membrane. All current tools assume bilayer is parallel to the xy plane.

With the basic model now constructed and evaluated further complexities can be added in order to more closely replicate the properties of synovial fluid and gain an understanding of the lubrication mechanism of synovial joints. Computational studies can provide the first steps and suggest relationships requiring experimental confirmation. Through building up by computation and narrowing in through experiment, a full understanding of lubrication of synovial joints can eventually be reached. With full understanding, new areas of study may open in joint disease treatment, prosthetics, and synthetic lubricants.

References

[1] Gary S. Firestein, Ralph C. Budd, Sherine E. Gabriel, Iain B. Mcinnes, and James R. O'dell.
Kelley's Textbook of Rheumatology.
Elsevier, 9th edition, 2013.

[2] OpenStax College.
Synovial joints.
Web Site, June 2013.
http://cnx.org/content/m46394/1.4/.

[3] B.A Hills and R.W Crawford.
Normal and prosthetic synovial joints are lubricated by surface-active phospholipid: a hypothesis.
The Journal of Arthroplasty, 18(4):499 – 505, 2003.

[4] Jayanth Katta, Zhongmin Jin, Eileen Ingham, and John Fisher.
Biotribology of articular cartilage a review of the recent advances.
Medical Engineering & Physics, 30(10):1349 – 1363, 2008.

[5] Marian W. Ropes, Alex F. Muller, and Walter Bauer.
The entrance of glucose and other sugars into joints.
Arthritis and Rheumatism, 3(6):496–514, 1960.

[6] J Currey, A Unsworth, and DA Hall.
Properties of bone, cartilage and synovial fluid.
Dowson D, Wright V (edited), An Introduction to the Biomechanics of Joints and Joint Replacement, Mechanical Engineering Publication, Suffolk, 1981.

[7] Ivonne Pasquali-Ronchetti, Daniela Quaglino, Giuseppe Mori, Barbara Bacchelli, and Peter Ghosh.
Hyaluronan phospholipid interactions.
Journal of Structural Biology, 120(1):1 – 10, 1997.

[8] R. Ionov, A. El-Abed, M. Goldmann, and P. Peretti.
Interactions of lipid monolayers with the natural biopolymer hyaluronic acid.
Biochimica et Biophysica Acta (BBA) - Biomembranes, 1667(2):200 – 207, 2004.

[9] Tannin A. Schmidt, Nicholas S. Gastelum, Quynhhoa T. Nguyen, Barbara L. Schumacher, and Robert L. Sah.
Boundary lubrication of articular cartilage: Role of synovial fluid constituents.
Arthritis & Rheumatism, 56(3):882–891, 2007.

[10] EL Radin, DA Swann, and PA Weisser.
Seperating hyluronate-free lubricating fraction from synovial fluie.
Nature, 288:377–378, October 1970.

[11] B.A. Hills and B.D. Butler.
Surfactants identified in synovial fluid and their ability to act as boundary lubricants.
Annals of Rheumatic Diseases, 43:641–648, 1984.

[12] David A Gibbs, EW Merrill, K Af Smith, and EA Balazs.
Rheology of hyaluronic acid.
Biopolymers, 6(6):777–791, 1968.

[13] Peter A Simkin and John E Bassett.
Cartilage matrix molecules in serum and synovial fluid.
Current opinion in rheumatology, 7(4):346–351, 1995.

[14] MJ How, VJW Long, and DR Stanworth.
The association of hyaluronic acid with protein in human synovial fluid.
Biochimica et Biophysica Acta (BBA)-Protein Structure, 194(1):81–90, 1969.

[15] David A Swann and Eric L Radin.
The molecular basis of articular lubrication i. purification and properties of a lubricating fraction from bovine synovial fluid.
Journal of Biological Chemistry, 247(24):8069–8073, 1972.

[16] IM Schwarz and BA Hills.
Surface-active phospholipid as the lubricating component of lubricin.
Rheumatology, 37(1):21–26, 1998.

[17] A Maroudas.
Balance between swelling pressure and collagen tension in normal and degenerate cartilage.
Nature, 260(5554):808–809, 1976.

[18] BP O'Hara, JP Urban, and A Maroudas.
Influence of cyclic loading on the nutrition of articular cartilage.
Annals of the rheumatic diseases, 49(7):536–539, 1990.

[19] Eric L Radin and Igor L Paul.
Response of joints to impact loading. i. in vitro wear.
Arthritis & Rheumatism, 14(3):356–362, 1971.

[20] BA Hills et al.
Oligolamellar lubrication of joints by surface active phospholipid.
The Journal of rheumatology, 16(1):82–91, 1989.

[21] Joseph L Rabinowitz, John R Gregg, James E Nixon, and H Ralph Schumacher.
Lipid composition of the tissues of human knee joints: I. observations in normal joints (articular cartilage, meniscus, ligaments, synovial fluid, synovium, intra-articular fat pad and bone marrow).
Clinical orthopaedics and related research, 143:260–265, 1979.

[22] Joseph L Rabinowitz, John R Gregg, and James E Nixon.

Lipid composition of the tissues of human knee joints: 11. synovial fluid in trauma. *Clinical orthopaedics and related research*, 190:292–298, 1984.

[23] Eric A. Smith and Phoebe K. Dea. Applications of calorimetry in a wide context - differential scanning calorimetry, isothermal titration calorimetry and microcalorimetry, 2013-01-23.

[24] RH Flores and MC Hochberg. Definition and classification of osteoarthritis. *Osteoarhtritis. Oxford: Oxford Medical Publications*, pages 1–12, 1998.

[25] DE Marcinko and MD Dollard. Physical and mechanical properties of joints (the pathomechanics of articular cartilage degeneration). *The Journal of foot surgery*, 25(1):3–13, 1985.

[26] John H Dumbleton. *Tribology of natural and artificial joints*, volume 3. Elsevier, 1981.

[27] Michael J Furey and Bettina M Burkhardt. Biotribology: Friction, wear, and lubrication of natural synovial joints. *Lubrication Science*, 9(3):255–271, 1997.

[28] Henry J Mankin and Louis Lippiello. The turnover of adult rabbit articular cartilage. *The Journal of Bone & Joint Surgery*, 51(8):1591–1596, 1969.

[29] HJ Mankin, KD Brandt, RW Moskowitz, VM Goldberg, and HJ Mankin. Osteoarthritis: diagnosis and management. *Saunders, Philadelphia, PA*, pages 43–80, 1984.

[30] CW McIlwraith and ANNE VACHON. Review of pathogenesis and treatment of degenerative joint disease. *Equine Veterinary Journal*, 20(s6):3–11, 1988.

[31] VC Mow and AF Mak. Lubrication of diarthrodial joints. *Handbook of bioengineering*, 5:1–5, 1987.

[32] D Dowson, V Wright, and MD Longfield. Human joint lubrication. *Biomedical engineering*, 4(4):160, 1969.

[33] SM Hsu and RS Gates. Boundary lubrication and boundary lubricating films. *Modern tribology handbook*, 1:455–492, 2001.

[34] A Erdemir. The role of hydrogen in tribological properties of diamond-like carbon films. *Surface and Coatings Technology*, 146:292–297, 2001.

[35] BA Hills. Surface-active phospholipid: a pandora?s box of clinical applications. part ii. barrier and lubricating properties. *Internal medicine journal*, 32(5-6):242–251, 2002.

[36] Manohar M Panjabi and Augustus A White. *Biomechanics in the musculoskeletal system*. Churchill Livingstone Philadelphia, 2001.

[37] Gerard A. Ateshian, Michael A. Soltz, Robert L. Mauck, Ines M. Basalo, Clark T. Hung, and W. Michael Lai. The role of osmotic pressure and tension-compression nonlinearity in the frictional response of articular cartilage. *Transport in Porous Media*, 50(1-2):5–33, 2003.

[38] Frank C Linn and Leon Sokoloff. Movement and composition of interstitial fluid of cartilage. *Arthritis & Rheumatism*, 8(4):481–494, 1965.

[39] Charles W McCutchen. Paper 1: Physiological lubrication. In *Proceedings of the Institution of Mechanical Engineers, Conference Proceedings*, volume 181, pages 55–62. SAGE Publications, 1966.

[40] BA Hills and MK Monds.
Enzymatic identification of the load-bearing boundary lubricant in the joint.
Rheumatology, 37(2):137–142, 1998.

[41] GD Jay and CJ Cha.
The effect of phospholipase digestion upon the boundary lubricating ability of synovial fluid.
The Journal of rheumatology, 26(11):2454–2457, 1999.

[42] T Little, MAR Freeman, and SAV Swanson.
Experiments on friction in the human hip joint.
Lubrication and wear in joints, page 110, 1969.

[43] Brian Andrew Hills.
The biology of surfactant.
Cambridge University Press, 1988.

[44] Gabrielle C Ballantine and Gwidon W Stachowiak.
The effects of lipid depletion on osteoarthritic wear.
Wear, 253(3):385–393, 2002.

[45] D Gvozdanovic, V Wright, and D Dowson.
Formation of lubricating monolayers at the cartilage surface.
Ann Rheum Dis, 34(suppl 2):100–1, 1975.

[46] AW Adamson and AP Gast.
The solid–liquid interface-contact angle.
Physical chemistry of surfaces, 4:333–361, 1997.

[47] M Priest, P Ehret, L Flamand, G Dalmaz, THC Childs, D Dowson, Y Berthier, AA Lubrecht, CM Taylor, and JM Georges.
Lubrication at the Frontier: The Role of the Interface and Surface Layers in the Thin Film and Boundary Regime, volume 36.
Elsevier, 1999.

[48] GT Barnes and IR Gentle.
An introduction to interfacial science, 2005.

[49] CM Larson and R Larson.
Standard Handbook of Lubrication, chapter Lubricant Additives, pages 14–1 – 14–22.
McGraw-Hill, 1969.

[50] RE Pattle.
The lining layer of the lung alveoli.
British medical bulletin, 19(1):41–44, 1963.

[51] Elwyn S Brown.
Isolation and assay of dipalmityl lecithin in lung extracts.
American Journal of Physiology–Legacy Content, 207(2):402–406, 1964.

[52] BA Hills, BD Butler, and RE Barrow.
Boundary lubrication imparted by pleural surfactants and their identification.
Journal of Applied Physiology, 53(2):463–469, 1982.

[53] BA Hills.
Oligolamellar nature of the articular surface.
The Journal of rheumatology, 17(3):349–356, 1990.

[54] D Guerra, L Frizziero, M Losi, B Bacchelli, G Mezzadri, and I Pasquali-Ronchetti.
Ultrastructural identification of a membrane-like structure on the surface of normal articular cartilage.
Journal of submicroscopic cytology and pathology, 28(3):385–393, 1996.

[55] BA Hills.
Boundary lubrication in vivo.
Proceedings of the Institution of Mechanical Engineers, Part H: Journal of Engineering in Medicine, 214(1):83–94, 2000.

[56] Bodo Purbach, Brian A Hills, and B Michael Wroblewski.
Surface-active phospholipid in total hip arthroplasty.
Clinical orthopaedics and related research, 396:115–118, 2002.

[57] Peter Ghosh, Nongporn Hutadilok, Naomi Adam, and Aldo Lentini.
Interactions of hyaluronan (hyaluronic acid) with phospholipids as determined by gel permeation chromatography, multi-

angle laser-light-scattering photometry and 1h-nmr spectroscopy.
International Journal of Biological Macromolecules, 16(5):237 – 244, 1994.

[58] V. Crescenzi, A. Taglienti, and I. Pasquali-Ronchetti.
Supramolecular structures prevailing in aqueous hyaluronic acid and phospholipid vesicles mixtures: an electron microscopy and rheometric study.
Colloids and Surfaces A: Physicochemical and Engineering Aspects, 245(1 - 3):133 – 135, 2004.

[59] LORNE RGale.
Biotribological assessment for artificial synovial joints: the role of boundary lubrication.
PhD thesis, School of Engineering Systems, Institute of Health and Biomedical Innovation (IHBI), Queensland University of Technology, 2007.

[60] A.-M. Trunfio-Sfarghiu, Y. Berthier, M.-H. Meurisse, and J.-P. Rieu.
Multiscale analysis of the tribological role of the molecular assemblies of synovial fluid. case of a healthy joint and implants.
Tribology International, 40(10 - 12):1500 – 1515, 2007.
Tribology at the Interface: Proceedings of the 33rd Leeds-Lyon Symposium on Tribology (Leeds, 2006).

[61] Siewert J Marrink, H Jelger Risselada, Serge Yefimov, D Peter Tieleman, and Alex H de Vries.
The martini force field: coarse grained model for biomolecular simulations.
The Journal of Physical Chemistry B, 111(27):7812–7824, 2007.

[62] Mario Orzi and Jonathan W. Essex.
The elba force field for coarse-grain modeling of lipid membranes.
PLoS ONE, 6(12), 2011.

[63] W Rawicz, KC Olbrich, T McIntosh, D. Needham, and E. Evans.
Effect of chain length and unsaturation on elasticity of lipid bilayers.
Biophysical Journal, 79(1):328–339, July 2000.

[64] Leonie Cowley.
Mechanical Role of Phospholipid Bilayers in Boundary Lubrication of Synovial Joints.
PhD thesis, University of Vermont, 2011.

[65] William Humphrey, Andrew Dalke, and Klaus Schulten.
VMD – Visual Molecular Dynamics.
Journal of Molecular Graphics, 14:33–38, 1996.

[66] John F Nagle and Stephanie Tristram-Nagle.
Structure of lipid bilayers.
Biochimica et Biophysica Acta (BBA)-Reviews on Biomembranes, 1469(3):159–195, 2000.

[67] Stephanie Tristram-Nagle, Horia I Petrache, and John F Nagle.
Structure and interactions of fully hydrated dioleoylphosphatidylcholine bilayers.
Biophysical journal, 75(2):917–925, 1998.

[68] Jianjun Pan, Stephanie Tristram-Nagle, Norbert Kučerka, and John F Nagle.
Temperature dependence of structure, bending rigidity, and bilayer interactions of dioleoylphosphatidylcholine bilayers.
Biophysical journal, 94(1):117–124, 2008.

[69] Yufeng Liu and John F Nagle.
Diffuse scattering provides material parameters and electron density profiles of biomembranes.
Physical Review E, 69(4):040901, 2004.

[70] Z Chen and RP Rand.
The influence of cholesterol on phospholipid membrane curvature and bending elasticity.
Biophysical journal, 73(1):267–276, 1997.

[71] Manfred Holz, Stefan R Heil, and Antonio Sacco.
Temperature-dependent self-diffusion coefficients of water and six selected molecular liquids for calibration in accurate 1h nmr pfg measurements.
Physical Chemistry Chemical Physics, 2(20):4740–4742, 2000.